Suppressed-to-enhanced thermal transport in a Fermi-Pasta-Ulam superlattice: Mediation roles of solitons and phonons

Jianjin Wang[1,2] and Jige Chen[2,3,*]

[1]*Department of Physics, Jiangxi Science & Technology Normal University, Nanchang 330013, China*
[2]*Zhangjiang Laboratory, Shanghai Advanced Research Institute, Chinese Academy of Sciences, Shanghai 201210, China*
[3]*Shanghai Institute of Applied Physics, Chinese Academy of Sciences, Shanghai 201800, China*

(Received 2 June 2019; revised manuscript received 16 September 2019; accepted 16 March 2020; published 14 April 2020)

Managing thermal transport in nanostructured materials possesses both theoretical and application value in thermoelectric and microelectronics design. Though a suppressed thermal conductivity could be easily achieved through disorder-induced phonon scattering in a superlattice, it is challenging to enhance thermal transport in a periodically designed lattice. In this paper, we show the possibility of mediating thermal conductivity from a suppressed to an enhanced value in a Fermi-Pasta-Ulam β superlattice with periodic cells of arithmetically increased nonlinearity. When the cell length is increased, thermal conductivity in the superlattice crosses over a suppressed region into an enhanced one and it is even higher than in a homogeneous lattice with the same nonlinearity strength. The mediation originates from the long-lived nonlinear wave packets as solitons across the disorder-induced interface between cells of the superlattice, while at the same time the normal vibrational modes as phonons are suppressed. Our result shows a promising strategy to manipulate thermal transport over a wide range in a superlattice with strong nonlinearity.

DOI: 10.1103/PhysRevE.101.042207

I. INTRODUCTION

Understanding thermal transport behavior in nanostructured materials like a semiconductor superlattice is a fundamental challenge for thermoelectric energy harvesting, heat dissipation, design of thermal logic gates and diodes, etc. [1–6]. For good performance of the thermoelectric materials, it is intensively studied for strategies to suppress thermal transport in a superlattice. Various experimental and theoretical works suggest an ultralow thermal conductivity of superlattices achieved by interfacial phonon scattering [7–13], band-gap-induced group velocity reduction [14,15], phonon resonance and filtering [16–18], broadband Anderson localization [19], etc. On the other hand, it is more challenging to achieve a high thermal conductivity in a superlattice because it is unlikely to avoid the intrinsic disorder at the interface of its periodic cell, which confers a strong thermal resistance to phonons. Dispersing one material into another one, the derived thermal conductivity is thus usually lower than the homogeneous counterpart. To our best knowledge, there have been very few studies that could enhance the thermal conductivity of a superlattice [20–22]. They use isotopes to flatten the phonon dispersion, where one particular structure might enhance the thermal conductivity under a large mass mismatch. Therefore, a new strategy is called for to evade the limit of phonons for adjustment of the thermal conductivity from suppression to enhancement in a superlattice.

As the temperature or nonlinearity is increased, energy carriers like solitons rather than phonons could be excited in classic lattices like the Fermi-Pasta-Ulam β (FPU-β) lattice with a nonlinear quartic term [3,4,23–32]. Preliminary research also suggests evidence of nonlinear energy carriers in some low-dimensional materials whose covalent bonds relate to strong nonlinearity, such as carbon nanotubes, graphene, and black phosphorene [33–41]. Solitons are surmised to play a significant role in anomalous thermal conduction and thermal rectification. In a perfect integrable system, scattering of solitons is elastic and no energy exchange occurs in the collisions of solitons with themselves and phonons [26,42–45]. Solitons are thus particularly robust in carrying thermal energy against interfacial disorder. Solitons rather than phonons were argued to be responsible for FPU recurrence over half a century ago [46,47]. Since then, there has been ongoing debate about the dominant energy carriers being solitons or phonons, with studies of the sound velocity, temperature dependence of the thermal conductivity, and phase shift of wave fronts in the FPU lattice [23–27,30–32]. This raises the reasonable expectation of soliton-mediated thermal behavior in a modified FPU lattice (FPU superlattice) as long as phonons can be suppressed due to the intrinsic disorder at the cell interface.

In this paper, we study thermal transport in an FPU-β superlattice with periodic cells of arithmetically increased nonlinear quartic coefficients and in disorder and homogeneous FPU-β lattices with the same nonlinearity strength. The thermal conductivity of the superlattice is dependent on its cell length, which reaches a minimum value at a certain length and then gradually increases to be higher than the value in the other two lattices. This variation is independent of the nonlinearity strength of the superlattice. By investigating the

*chenjige@zjlab.org.cn

 ©2020 American Physical Society

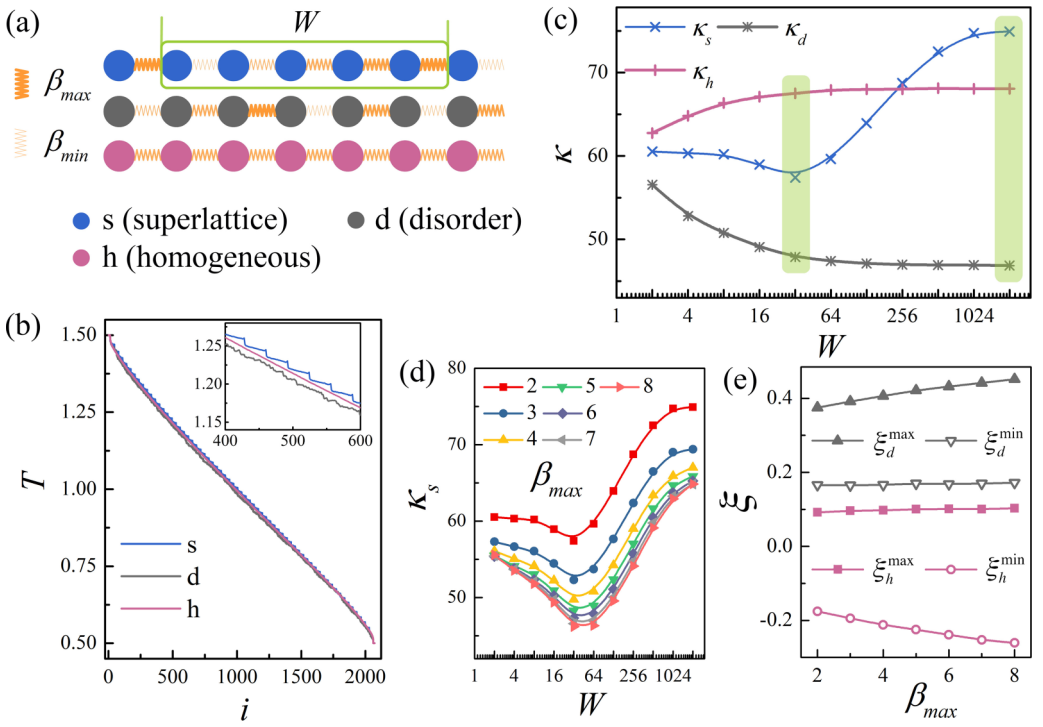

FIG. 1. (a) Schematic of an FPU-β superlattice (upper, blue lattice) with arithmetically increased nonlinear quartic coefficients from $\beta_{\min}$ to $\beta_{\max}$ in its periodic cell of length W, a disorder lattice (middle, gray lattice) with randomly distributed quartic coefficients between $\beta_{\min}$ and $\beta_{\max}$, and a homogeneous lattice (bottom, red lattice) with an averaged quartic coefficient $\langle\beta\rangle = (\beta_{\min} + \beta_{\max})/2$. (b) Temperature gradient of the three superlattice systems with the nonlinear strength at $W = 32$ and $\beta_{\max} = 2$ [upper, blue line, of the superlattice (s); bottom, gray line, of the disordered lattice (d); and middle, red line, of the homogeneous lattice (h)]. (c) Thermal conductivity of a superlattice κ_s (middle, blue line with x's), a disorder lattice κ_d (bottom, gray line with asterisks), and a homogeneous lattice κ_h (upper, red line with crosses), with $\beta_{\max} = 2$, as a function of W. Green-shaded boxes indicate the minimum and maximum thermal conductivity in the superlattice at $W = 32$ and $W = 2048$. (d) κ_s of $\beta_{\max} = 2$–8 in a periodic cell (indicated by lines with different symbols). (e) Variation ratio of the minimum and maximum difference between the disorder lattice and the superlattices $\xi_d^{\min}$ (gray line with open downward triangles) and $\xi_d^{\max}$ (gray line with filled upward triangles), and between the homogeneous lattice and the superlattices $\xi_h^{\min}$ (red line with open circles) and $\xi_h^{\max}$ (red line with filled squares), as a function of $\beta_{\max}$.

dynamics of phonons and solitons, it is found that long-lived solitons and suppressed phonons determine the suppressed-to-enhanced thermal conductivity.

II. METHODS

A schematic of the three lattice systems is shown in Fig. 1(a), where three lattice systems, namely, an FPU-β superlattice and disorder and homogeneous lattices with the same nonlinearity strength, are studied. The adopted FPU lattice model is given by its dimensionless Hamiltonian as [26,27,29,30],

$$H = \sum_{i=1}^{N}\left[\frac{p_i^2}{2} + \frac{(q_{i+1}-q_i)^2}{2} + \frac{\beta_i(q_{i+1}-q_i)^4}{4}\right], \quad (1)$$

where p_i denotes the momentum and q_i denotes the displacement-from-equilibrium position of the ith atom, N is the total lattice length, and $N = 2048$. The superlattice is characterized by two independent parameters, i.e., the cell length W and the maximum quartic coefficient $\beta_{\max}$. The quartic coefficient arithmetically increases from $\beta_{\min} = \beta_{\max}/W$ to $\beta_{\max}$ in the periodic cell as an arithmetic sequence with a common difference of $\beta_{\max}/W$. The comparative disorder and homogeneous lattices are also characterized by W and $\beta_{\max}$. The lattice is one supercell with $W = N$. The supercell repeats once with $W = N/2$, which refers to the theoretical limit of a superlattice. The quartic term is randomly distributed as $\beta_i \in [\beta_{\min}, \beta_{\max}]$ in the disorder lattice, while it is the same as $\beta_i = (\beta_{\min} + \beta_{\max})/2$ in the homogeneous lattice. Two Nosé-Hoover heat baths with 24 extra atoms are coupled to the two ends of the lattices as a heat source, $T_H = 1.5$, and a heat sink, $T_L = 0.5$. The quartic term in the heat baths is fixed as the last one in the lattice to avoid the boundary effect (e.g., in the superlattice, $\beta_i = \beta_{\min}$ in the heat source and $\beta_i = \beta_{\max}$ in the heat sink). Fourier' s law is applied to calculate the thermal conductivity κ as [4]

$$\kappa = \frac{J}{(T_H - T_L)/N},$$
$$J = \left\langle \frac{1}{2}(\dot{q}_{i+1} + \dot{q}_i)\frac{\partial H(q_{i+1}-q_i)}{\partial q_i}\right\rangle, \quad (2)$$
$$\frac{\partial H(q_{i+1}-q_i)}{\partial q_i} = -(q_{i+1}-q_i) - 3\beta_i(q_{i+1}-q_i)^3,$$

where J is the heat current, $\langle\cdot\rangle$ denotes the ensemble averages, and $\partial H(q_{i+1}-q_i)/\partial q_i$ refers to the atomic force

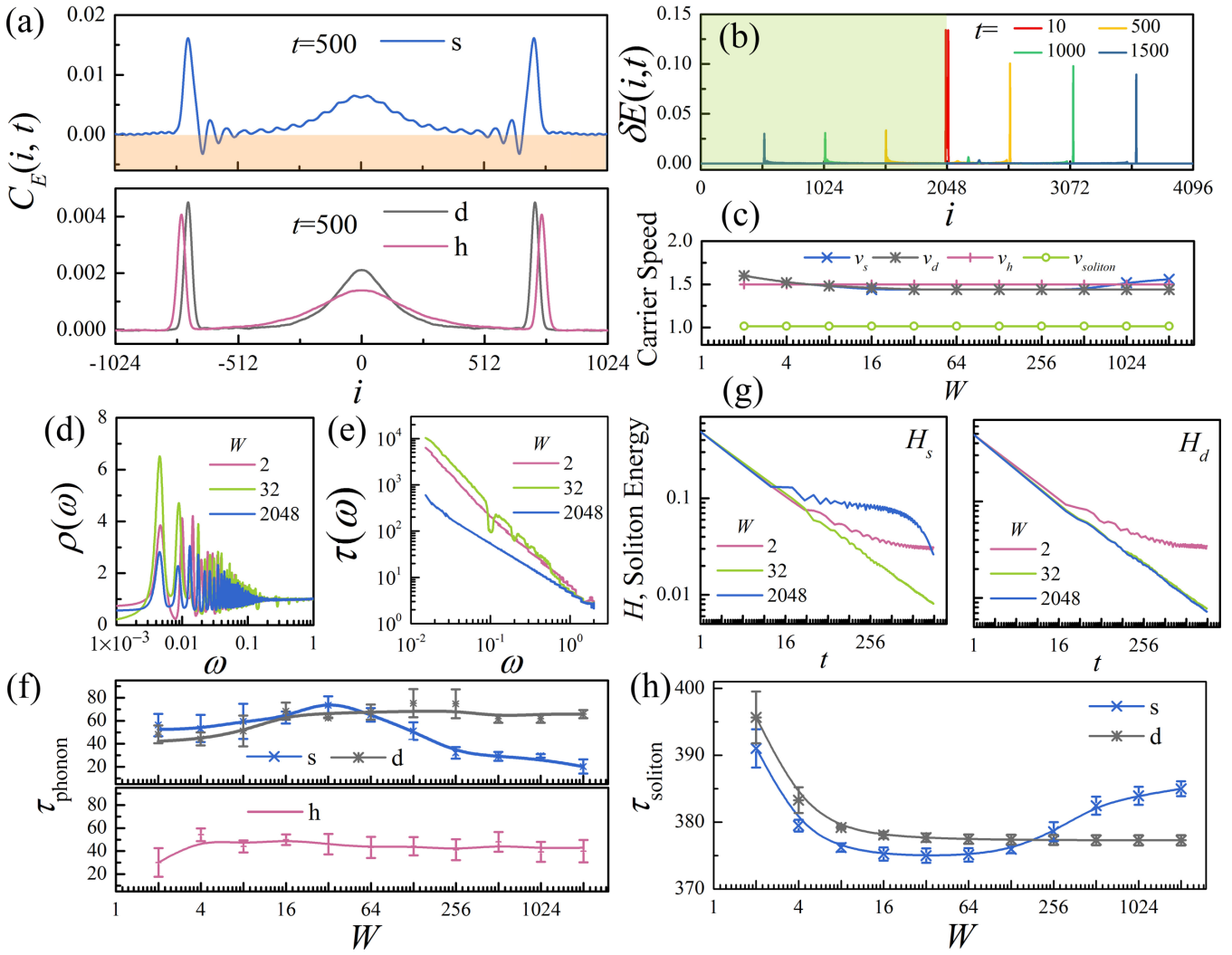

FIG. 2. (a) Energy correlation $C_E(i,t)$ of a superlattice (s), disorder lattice (d; gray line with a higher center peak), and homogeneous lattice (h; red line with a smaller center peak) at $t = 500$ for temperature $T = 1$ and $W = 32$. The orange-shaded area implies a negative regime of $C_E(i,t)$. (b) Time variations of an energy excitation $\delta E(i,t)$ along the superlattice (green-shaded area) and along an extended homogeneous lattice for an initial pulse $H_{2048}(0) = 1$ and $W = 2$ at $T = 0$. (c) Speed of phonons v_s in the superlattice (upper, blue line with x's), v_d (upper, gray line with asterisks) in the disorder lattice, and v_h in the homogeneous lattice (upper, red line with crosses) and speed of solitons v_{soliton} (bottom, green line with open circles) excited by $H_{2048}(0) = 1$ as a function of W. (d, e) Phonon density distributions $\rho(\omega)$ and lifetime distributions $\tau(\omega)$ as a function of the frequency ω in the superlattice ($W = 2$, red line; $W = 32$, green line; and $W = 2048$, blue line). (f) Average phonon lifetime τ_{phonon} as a function of W in the three lattice systems (superlattice—upper, blue line with x's; disordered lattice—upper, gray line with asterisks; and homogeneous lattice—bottom, red line). (g) Decay of soliton energy H_s in the superlattice and H_d in the disorder lattice with time ($W = 2$, red line; $W = 32$, green line; and $W = 2048$, blue line). (h) Average soliton lifetimes τ_{soliton} as a function of W in the superlattice and disorder lattice (superlattice, blue line with x's; disordered lattice, gray line with asterisks).

of the ith atom implemented on the $(i+1)$th atom. The thermal conductivity of the superlattice is denoted κ_s, the thermal conductivity of the disorder lattice is denoted κ_d, and the thermal conductivity of the homogeneous lattice is denoted κ_h.

III. RESULTS AND DISCUSSION

The typical temperature profiles of a superlattice of $W = 32$ and $\beta_{\max} = 2$ and of disorder and homogeneous lattices with the same nonlinearity are illustrated in Fig. 1(b). The intrinsic disorder at the interface of the periodic cell leads to a temperature discontinuity at the cell ends, which represents the intrinsic thermal resistance to phonons. Later similar discontinuities in energy correlations are shown in Fig. 2(a). A random temperature disorder and a perfect linear temperature variation are observed in the disorder and homogeneous lattices.

The typical variations of κ in the three lattice systems as a function of W are illustrated in Fig. 1(c), where $W = 2$–2048 (in the form of 2^x) and $\beta_{\max} = 2$. The variations in the disorder and homogeneous lattices are simple; κ_d decreases from its maximum value 56.55 at $W_0 = 2$ to its minimum value 46.85 at $W_2 = 2048$, and κ_h increases from its minimum value 62.75 at $W_0 = 2$ to its maximum value 68.06 at $W_2 = 2048$. The superlattice exhibits a nonmonotonic variation of κ_s, where it

first decreases from its peak value 60.53 at $W_0 = 2$ to its minimum value 57.41 at $W_1 = 32$, and then gradually increases to its maximum value 74.92 at $W_2 = 2048$. Interestingly, the thermal conductivity of the superlattice is always higher than that of the disorder lattice, as $\kappa_s > \kappa_d$, while it is not always smaller than its homogeneous counterpart, as $\kappa_s < \kappa_h$ ($W \leqslant 128$) and $\kappa_s > \kappa_h$ ($W \geqslant 256$). This unexpected mediation from suppression to enhancement reveals the possibility of flexible thermal management.

The thermal conductivity κ_s of the superlattice is adjustable by the nonlinearity strength with $\beta_{\max}$ from 2 to 8. As illustrated in Fig. 1(d), the minimum and maximum values of the superlattice always occur at the same cell length, $W_1 = 32$ and $W_2 = 2048$, with different $\beta_{\max}$ values (variations of κ_d and κ_h with $\beta_{\max}$ are shown in PS1 in the Supplemental Material [48]). To characterize the suppression and enhancement of κ_s as a function of $\beta_{\max}$, we use the difference ratio of its extreme values between the disorder and the homogeneous lattices as

$$\xi_d^{\min} = \frac{\kappa_s(W_1) - \kappa_d(W_1)}{\kappa_s(W_1)}, \quad \xi_d^{\max} = \frac{\kappa_s(W_2) - \kappa_d(W_2)}{\kappa_s(W_2)},$$
$$\xi_h^{\min} = \frac{\kappa_s(W_1) - \kappa_h(W_1)}{\kappa_s(W_1)}, \quad \xi_h^{\max} = \frac{\kappa_s(W_2) - \kappa_h(W_2)}{\kappa_s(W_2)}, \quad (3)$$

where $\kappa_s(W_1)$ and $\kappa_s(W_2)$ refer to the minimum and maximum values. The four ratios $\xi_d^{\min}$, $\xi_d^{\max}$, $\xi_h^{\min}$, and $\xi_h^{\max}$ could serve as comparative quantities to illustrate the changes due to nonlinearity strength between the superlattice and the other two lattice systems. As shown in Fig. 1(e), four linear relations are obtained. Comparing with the disorder lattice, it is obtained that $\xi_d^{\min} = 0.17$ and $\xi_d^{\max} = 0.35 + 0.013\beta_{\max}$, which refer to the same suppression in both lattice systems at W_1 and a linear enhancement in the superlattice at W_2. Comparing with the homogeneous lattice, it is obtained that $\xi_h^{\min} = -0.15 - 0.014\beta_{\max}$ and $\xi_h^{\max} = 0.098$, which refer to a linear suppression in the superlattice at W_1 and the same enhancement in both lattice systems at W_2. The suppression ratio ($-0.014\beta_{\max}$) and enhancement ratio ($0.013\beta_{\max}$) are quite close, which implies the same microscopic mechanism in governing the thermal transport mediation.

Consistently, we have also considered the thermal conductivity variations by varying the lattice lengths. We find similar suppressed-to-enhanced mediation by decreasing or increasing the lattice lengths in the three lattice systems (please see variations of κ_s, κ_d, and κ_h with $N = 512$ and 4096 in the Supplemental Material [48]). Interestingly, it is also found that superlattice systems with different W values exhibit similar logarithm increases: $\kappa_s \sim 9.56 \log_2 N$ ($W = 2$), $\kappa_s \sim 9.52 \log_2 N$ ($W = 32$), and $\kappa_s \sim 9.73 \log_2 N$ ($W = 512$). The logarithm dependence of the thermal conductivity on the lattice length indicates a strong anomalous thermal conductivity divergence due to the enhanced nonlinearity strength in the FPU superlattice. The logarithm dependence of the thermal conductivity on the lattice length of the superlattice was similarly found in a two-dimensional FPU disk model [49]. There is also no thermal rectification effect in the superlattice upon changing the increased nonlinearity to be decreased nonlinearity in its cell (please see κ_s' in the Supplemental Material [48]).

To understand the microscopic origin of this suppressed-to-enhanced mediation in the superlattice, we study the dynamics of the energy carriers, namely, the speed and scattering of phonons and solitons. Phonons as harmonic vibrational modes could be extracted from fluctuations while solitons are masked by fluctuations in thermal equilibrium. Therefore, conventionally, the equilibrium calculations are applied to identify the properties of phonons, while the momentum excitations in the static lattice are applied for solitons [25,26,31,32]. First, time variations in the energy correlation $C_E(i,t)$ [27,29,30] and energy excitation $\delta E(i,t)$ [26,28,40,41] are calculated to get the spatiotemporal spreading of an initial energy fluctuation as

$$C_E(i,t) = \frac{\langle \Delta H_i(t) \Delta H_0(0) \rangle}{\langle \Delta H_0(0) \Delta H_0(0) \rangle}, \quad \Delta H_i(t) = H_i(t) - \langle H_i(t) \rangle, \quad (4)$$

$$\delta E(i,t) = H_i^{\text{ext}}(t) - H_i^{\text{nonext}}(t), \quad (5)$$

where $C_E(i,t)$ is calculated in an equilibrium ensemble at temperature $T = 1$. $H_i(t)$ refers to the total energy of the ith atom at time t. $H_i^{\text{ext}}(t)$ refers to the total energy of the ith atom at time t, which starts from the initial condition of a pulse $H_{2048}(0)$ by adding the atomic velocity $v_{2048}(0) = -\sqrt{2H_{2048}(0)}$ at time $t = 0$ and temperature $T = 0$. $H_i^{\text{nonext}}(t)$ refers to the total energy of the ith atom at time t, which starts from an initial condition without any pulses at temperature $T = 0$, and $H_i^{\text{nonext}}(t) = 0$ in the FPU lattice systems. $C_E(i,t)$ could be used to describe the speed of phonons by measuring the peak positions of the propagating fronts, while $\delta E(i,t)$ could be used to describe the speed of solitons by measuring the excited solitary wave fronts. As illustrated in Fig. 2(a), the speeds of phonons are almost identical for $W = 32$ in the three lattice systems, where $v_s = 1.45$ in the superlattice, $v_d = 1.45$ in the disorder lattice, and $v_h = 1.50$ in the homogeneous lattice (please see the time variations of $C_E(i,t)$ in the Supplemental Material [48]). Figure 2(c) shows that the speed of phonons is insensitive to W in the three lattice systems (their differences are within 3%). Discontinuity at the cell interface of the superlattice is observed in $C_E(i,t)$, which represents its intrinsic arithmetical correlation ($C_E(i,t)$ values of all W's are illustrated in the Supplemental Material [48]). The negative regime observed in the superlattice excludes $C_E(i,t)$ as a probability distribution. Meanwhile, as illustrated in Fig. 2(b), two solitons, excited by an initial pulse $H_{2048}(0) = 1$, transport along the superlattice of $W = 2$ from right to left ($v_{\text{soliton}} = 1.02$) and along the extended homogeneous lattice in the opposite direction ($v_{\text{soliton}} = 1.03$). As illustrated in Fig. 2(c), the speed of solitons v_{soliton} is identical in the three lattice systems and insensitive to W ($v_{\text{soliton}} > 1$, and it is dependent on its energy as illustrated in the Supplemental Material [48]). As a result, it implies that thermal mediation does not originate from carrier speed variations.

Next, the phonon power spectrum $\rho(\omega)$ and lifetime spectrum $\tau(\omega)$ are calculated to estimate the average lifetime of phonons τ_{phonon}. The time variation of soliton energy decay is calculated to estimate the average lifetimes of solitons τ_{soliton}.

In the superlattice, they are calculated as [50,51]

$$\rho(\omega) = \frac{1}{2\pi}\int \langle v_i(t)v_i(0)\rangle e^{-i\omega t}dt \tag{6}$$

$$\tau(\omega) = \frac{1}{1-\frac{1}{e}}\int_0^{t_c} \frac{\langle \Delta H_\omega(t)\Delta H_\omega(0)\rangle}{\langle \Delta H_\omega(0)\Delta H_\omega(0)\rangle}dt,$$

$$\Delta H_\omega(t) = H_\omega(t) - \langle H_\omega(t)\rangle, \tag{7}$$

$$\tau_{\text{phonon}} = \frac{\int \tau(\omega)\rho(\omega)d\omega}{\int \rho(\omega)d\omega}, \tag{8}$$

$$H_s(t) = \sum_{i\in soliton} \delta E(i,t), \quad \tau_{\text{soliton}} = \left\langle \frac{NH_s(0)}{\partial H_s(t)/\partial t}\right\rangle. \tag{9}$$

For calculations of phonons, $v_i(t) = \dot{q}_i(t)$ and $v_i(0) = \dot{q}_i(0)$ are the velocities of the ith atom at times t and 0, and $\Delta H_\omega(t)$ is the energy fluctuation of a phonon mode ω. For each phonon mode ω_k, its energy is calculated by $H_{\omega_k} = \frac{1}{2}(P_k^2 + \omega_k^2 Q_k^2)$, and $P_k = \sum_{i=1}^N \sqrt{m_i}v_i V_i^k = \sum_{i=1}^N v_i V_i^k$ and $Q_k = \sum_{i=1}^N \sqrt{m_i}q_i V_i^k = \sum_{i=1}^N q_i V_i^k$ are the relative canonical momentum and canonical coordinate. The lifetime of phonons is derived based on the single-mode relaxation time approximation. Under this approximation, a relaxation time is assigned to each phonon mode and it represents the temporal response of the lattice due to the particular activated phonon mode. Therefore, as discussed in the literature [51,52], the lifetime of a particular phonon mode can be defined by the time integral of the autocorrelation of its energy fluctuation from the equilibrium value. Since the autocorrelation decays exponentially, the infinite time integral of calculating the phonon lifetime $\tau(\omega)$ could be numerically cut off at a particular small value. In our calculations, the cutoff value of the time integral is selected to be t_c where the autocorrelation is smaller than $1/e$, and τ_{phonon} is calculated by averaging the lifetime of all 2048 phonon modes. Calculation details for each phonon mode are discussed in the Supplemental Material [48].

For calculation of solitons, $H_s(t)$ is the energy of a soliton at time t, $H_s(0)$ is its initial energy, and $N = 2048$ is the lattice length. Here $i \in soliton$ indicates that the summation is performed over the width of the solitons (usually it crosses about 8–10 lattice sites) [26,45]. Since solitons are supersonic and strongly centralized, $\delta E(i,t) = 0$ when the summation is out of the range of the solitons. The decay procedure of a soliton by propagating from its excitation point (the right end of the superlattice) to the other side boundary (the left end of the superlattice) provides a numerical measure to compare its robustness to the interfacial disorder in the superlattice. The lifetime of solitons in the superlattice could be numerically compared by τ_{soliton}. τ_{soliton} is calculated by averaging the lifetime of solitons excited by an initial pulse $H_{2048}(0)$ from 0.875 [$v_{2048}(0) = -\sqrt{2H_{2048}(0)} = -1.32$] to 1.125 [$v_{2048}(0) = -1.5$] within the time N/v_{soliton}. τ_{soliton} denotes the average lifetime in which a soliton would decay to be its averaged energy after propagating from one end to another in the lattice.

Typical $\rho(\omega)$ and $\tau(\omega)$ values of the superlattice are shown in Figs. 2(d) and 2(e), and the average lifetimes of phonons in the three lattice systems are illustrated in Fig. 2(f). Interestingly, compared with the variation of κ_s in Fig. 1(c), a complete opposite variation of τ_{phonon} is observed in the superlattice as a function of W, where the maximum τ_{phonon} occurs at $W = 32$ and two minimum τ_{phonon} occur, at $W = 2$ and 2048. Similar opposite variations between τ_{phonon} and κ_d are observed in the disorder lattice. Meanwhile, soliton decay in the superlattice and the disorder lattice are illustrated in Fig. 2(g) (it is negligible in the homogeneous lattice without interfacial disorder). Compared with the exponential decay of phonons, the decay is very slow (slower than a power-law decay) due to the particlelike nature of solitons. For example, in the superlattice with $W = 2$, a soliton exhibits a slow power-law decay at first ($t < 256$) and then the decay is negligible in the following time (scattering of solitons with other W's are illustrated in the Supplemental Material [48]). Similar behavior of solitons is observed in the disorder lattice. The lifetimes of solitons τ_{soliton} as a function of W in the superlattice and disorder lattice are illustrated in Fig. 2(h), where perfect agreement with the variation of κ_s and κ_d is observed. The negative (totally opposite) predication from phonons and the positive predication from solitons imply the long-lived solitons rather than the suppressed phonons as the microscopic mechanism of the thermal conduction mediation in the superlattice and disorder lattice. The homogeneous lattice relates to the usual FPU model in the literature. The phonon-mediated variation indicates that thermal transport is more determined by phonons if no interfacial scattering occurs. On the other hand, if phonons were suppressed by the interfacial scattering, solitons would become the dominant energy carriers in the FPU lattice.

Here we would like to emphasize that, in this paper, the analysis of phonons is under the harmonic approximation. A linearized algebra equation is derived for each atom to solve the eigenvalue of the dynamic matrix and thus phonons refer to the classic definition as discrete harmonic oscillation modes. The nonlinear effect is considered in the single-mode relaxation time approximation of phonons and the analysis of solitons. It is different from the effective (renormalized) phonon approximation [30], where the mean-field treatment of nonlinear terms of each atom is used to renormalize the eigenvalue (eigenfrequency) of phonons. Meanwhile, we are aware that disorder-induced localization could lead to an absence of diffusion of waves in a lattice with sufficiently large randomness (usually, of mass) and consistently affect thermal transport in nonlinear lattices. It is known that disorder of mass would destabilize solitons, while strong nonlinearity would reduce Anderson localization [19,53]. Therefore, it would be extremely difficult to clearly distinguish the contribution of localization to lattices with disordered nonlinearity rather than mass. In this paper, we focus our attention on elaborating the contributions of solitons and phonons to the thermal mediation. By comparison with the homogeneous and superlattice cases, it would be helpful to know that, in the disordered lattice, the lifetime of solitons exhibits a tendency to decay and the lifetime of phonons exhibits a tendency to be prolonged when the cell length is increased. The explicit role of the localization effect remains for future study. Furthermore, the in-band discrete breathers within the phonon frequency are unstable and would rapidly decay in a nonlinear lattice [54–56]. In-band discrete breathers are usually found in lattice systems with both nearest- and next-nearest-neighbor interactions [57,58]. Since only nearest interactions

are considered in our lattice model, we think that the unstable discrete breathers are unlikely to affect our numerical analysis of phonons using the parameters in this paper.

IV. CONCLUSION

In summary, we find suppressed-to-enhanced thermal conductivity mediation in an FPU-β superlattice with periodic cells of arithmetically increased nonlinearity. The dynamics of energy carriers, i.e., phonons and solitons, are calculated to understand the microscopic mechanism. It is found that the long-lived solitons and suppressed phonons across the disordered interface determine the enhanced thermal conductivity in the superlattice. Similar soliton-enhanced and the usual phonon-mediated thermal transport behaviors are observed in disorder and homogeneous lattices. Our finding implies a new strategy to achieve suppressed-to-enhanced thermal conductivity in a superlattice through long-lived nonlinear energy carriers like solitons.

ACKNOWLEDGMENTS

This work was supported by the National Natural Science Foundation of China (Grants No. 11405245 and No. 11847015), Natural Science Foundation of Shanghai (Grants No. 14ZR1448100 and No. 19ZR1463200), and Start-up Fund of Jiangxi Science and Technology Normal University (Grant No. 2017BSQD002). The authors also thank the Shanghai Supercomputer Center of China and the Supercomputing Center of the Chinese Academy of Sciences.

[1] N. Li, J. Ren, L. Wang, G. Zhang, P. Hanggi, and B. Li, Rev. Mod. Phys. **84**, 1045 (2012).
[2] M. Maldovan, Nature **503**, 209 (2013).
[3] A. Dhar, Adv. Phys. **57**, 457 (2008).
[4] S. Lepri, R. Livi, and A. Politi, Phys. Rep. **377**, 1 (2003).
[5] B. Li, L. Wang, and G. Casati, Phys. Rev. Lett. **93**, 184301 (2004).
[6] L. Wang and B. Li, Phys. Rev. Lett. **99**, 177208 (2007).
[7] M. V. Simkin and G. D. Mahan, Phys. Rev. Lett. **84**, 927 (2000).
[8] G. Pernot *et al.*, Nat. Mater. **9**, 491 (2010).
[9] J.-K. Yu, S. Mitrovic, D. Tham, J. Varghese, and J. R. Heath, Nat. Nano **5**, 718 (2010).
[10] Y. Chalopin, K. Esfarjani, A. Henry, S. Volz, and G. Chen, Phys. Rev. B **85**, 195302 (2012).
[11] J. Ravichandran *et al.*, Nat. Mater. **13**, 168 (2013).
[12] P. Hołuj *et al.*, Phys. Rev. B **92**, 125436 (2015).
[13] Y. Liao, T. Shiga, M. Kashiwagi, and J. Shiomi, Phys. Rev. B **98**, 134307 (2018).
[14] M. Hu and D. Poulikakos, Nano Lett. **12**, 5487 (2012).
[15] J. Garg and G. Chen, Phys. Rev. B **87**, 140302(R) (2013).
[16] D. L. Nika, E. P. Pokatilov, A. A. Balandin, V. M. Fomin, A. Rastelli, and O. G. Schmidt, Phys. Rev. B **84**, 165415 (2011).
[17] M. Maldovan, Nat. Mater. **14**, 667 (2015).
[18] S. Xiong, K. Saaskilahti, Y. A. Kosevich, H. Han, D. Donadio, and S. Volz, Phys. Rev. Lett. **117**, 025503 (2016).
[19] T. Juntunen, O. Vanska, and I. Tittonen, Phys. Rev. Lett. **122**, 105901 (2019).
[20] D. A. Broido and T. L. Reinecke, Phys. Rev. B **70**, 081310(R) (2004).
[21] A. Ward and D. A. Broido, Phys. Rev. B **77**, 245328 (2008).
[22] J. Garg, N. Bonini, and N. Marzari, Nano Lett. **11**, 5135 (2011).
[23] N. Theodorakopoulos and M. Peyrard, Phys. Rev. Lett. **83**, 2293 (1999).
[24] K. Aoki and D. Kusnezov, Phys. Rev. Lett. **86**, 4029 (2001).
[25] B. Hu, B. Li, and H. Zhao, Phys. Rev. E **61**, 3828 (2000).
[26] H. Zhao, Z. Wen, Y. Zhang, and D. Zheng, Phys. Rev. Lett. **94**, 025507 (2005).
[27] H. Zhao, Phys. Rev. Lett. **96**, 140602 (2006).
[28] G. Kopidakis, S. Komineas, S. Flach, and S. Aubry, Phys. Rev. Lett. **100**, 084103 (2008).
[29] S. Liu, P. Hanggi, N. Li, J. Ren, and B. Li, Phys. Rev. Lett. **112**, 040601 (2014).
[30] N. Li, B. Li, and S. Flach, Phys. Rev. Lett. **105**, 054102 (2010).
[31] Y. Ming, L. Ye, D.-B. Ling, H.-S. Chen, H.-M. Li, and Z.-J. Ding, Phys. Rev. E **98**, 032215 (2018).
[32] Y. Ming, L. Ye, H.-S. Chen, S.-F. Mao, H.-M. Li, and Z.-J. Ding, Phys. Rev. E **97**, 012221 (2018).
[33] T. Y. Astakhova, O. D. Gurin, M. Menon, and G. A. Vinogradov, Phys. Rev. B **64**, 035418 (2001).
[34] T. Y. Astakhova, M. Menon, and G. A. Vinogradov, Phys. Rev. B **70**, 125409 (2004).
[35] C. W. Chang, D. Okawa, A. Majumdar, and A. Zettl, Science **314**, 1121 (2006).
[36] A. V. Savin and Y. S. Kivshar, Europhys. Lett. **89**, 46001 (2010).
[37] Q. Bao and K. P. Loh, ACS Nano **6**, 3677 (2012).
[38] Y. Guo and W. Guo, Nanoscale **5**, 318 (2013).
[39] J. Chen, W. Qi, M. Zhang, and H. Zhao, J. Stat. Mech. (2015) P06007.
[40] J. Chen, S. Chen, and Y. Gao, J. Phys. Chem. Lett. **7**, 2518 (2016).
[41] J. Chen, S. Chen, and Y. Gao, Phys. Rev. B **95**, 134301 (2017).
[42] H. Ikezi, R. J. Taylor, and D. R. Baker, Phys. Rev. Lett. **25**, 11 (1970).
[43] P. G. Drazin and R. S. Johnson, *Solitons: An Introduction*, 2nd ed. (Cambridge University Press, Cambridge, UK, 1989).
[44] E. Arevalo, F. G. Mertens, Y. Gaididei, and A. R. Bishop, Phys. Rev. E **67**, 016610 (2003).
[45] T. Jin, H. Zhao, and B. Hu, Phys. Rev. E **81**, 037601 (2010).
[46] N. J. Zabusky and M. D. Kruskal, Phys. Rev. Lett. **15**, 240 (1965).
[47] E. Fermi, J. Pasta, and S. Ulam, Los Alamos National Laboratory Report No. LA-1940 (LANL, Los Alamos, NM, 1955).
[48] See Supplemental Material at http://link.aps.org/supplemental/10.1103/PhysRevE.101.042207 for more figures and information.
[49] D. Xiong, J. Wang, Y. Zhang, and H. Zhao, Phys. Rev. E **82**, 030101(R) (2010).
[50] J. M. Dickey and A. Paskin, Phys. Rev. **188**, 1407 (1969).

[51] A. J. C. Ladd, B. Moran, and W. G. Hoover, Phys. Rev. B **34**, 5058 (1986).
[52] A. J. H. McGaughey and M. Kaviany, Phys. Rev. B **69**, 094303 (2004).
[53] G. S. Zavt, M. Wagner, and A. Lutze, Phys. Rev. E **47**, 4108 (1993).
[54] A. J. Sievers and S. Takeno, Phys. Rev. Lett. **61**, 970 (1988).
[55] G. P. Tsironis and S. Aubry, Phys. Rev. Lett. **77**, 5225 (1996).
[56] G. P. Tsironis, A. R. Bishop, A. V. Savin, and A. V. Zolotaryuk, Phys. Rev. E **60**, 6610 (1999).
[57] R. Lai, S. A. Kiselev, and A. J. Sievers, Phys. Rev. B **56**, 5345 (1997).
[58] D. Xiong, J. Wang, Y. Zhang, and H. Zhao, Phys. Rev. E **85**, 020102(R) (2012).